Coded Aperture-Based Self-wavefront Interference Using Transverse Splitting Holography

Narmada Joshi
Institute of Physics,
University of Tartu,
Estonia.
narmada@ut.ee

Agnes Pristy Ignatius Xavier
Institute of Physics,
University of Tartu,
Estonia.
School of Electrical and Computer Engineering,
Ben Gurion University of the Negev,
Israel.
agnes.pristy.ignatius.xavier@ut.ee

Francis Gracy Arockiaraj
Institute of Physics,
University of Tartu,
Estonia.
School of Electrical and Computer Engineering,
Ben Gurion University of the Negev,
Israel.
francis.gracy.arockiaraj@ut.ee

Aravind Simon John Francis Rajeswary
Institute of Physics,
University of Tartu,
Estonia.
aravind@ut.ee

Saulius Juodkazis
Optical Sciences Center and ARC Training Centre in Surface Engineering for Advanced Materials (SEAM),
Swinburne University of Technology,
Australia.
Tokyo Tech World Research Hub Initiative (WRHI), School of Materials and Chemical Technology,
Tokyo Institute of Technology,
Japan.
sjuodkazis@swin.edu.au

Joseph Rosen
School of Electrical and Computer Engineering,
Ben-Gurion University of the Negev,
8410501, Beer-Sheva,
Israel.
Institute of Physics,
University of Tartu,
Estonia.
rosenj@bgu.ac.il

Aile Tamm
Institute of Physics,
University of Tartu,
Estonia.
Aile.Tamm@hm.ee

Vijayakumar Anand
Institute of Physics,
University of Tartu,
Estonia.
Optical Sciences Center and ARC Training Centre in Surface Engineering for Advanced Materials (SEAM),
School of Science, Computing and Engineering Technologies,
Swinburne University of Technology,
Hawthorn, Melbourne, VIC 3122,
Australia.
vijayakumar.anand@ut.ee

2023 International Conference on Next Generation Electronics (NEleX) | 979-8-3503-1908-8/23/$31.00 ©2023 IEEE | DOI: 10.1109/NELEX59773.2023.10421591

***Abstract*—Self-wavefront interference transverse splitting holography (SWITSH) is a recently developed holographic technique to solve a fundamental problem in the manufacturing of large-area diffractive lenses. In SWITSH, a low NA diffractive lens modulates the light from an object, and the modulated light is interfered with light from the same object that reaches beyond the aperture of the diffractive lens. The resulting self-interference hologram is processed with the pre-recorded point spread hologram using the Lucy-Richardson-Rosen algorithm. Since the self-interference hologram is formed by collecting light beyond the NA of the diffractive lens, it acquires the object information corresponding to the higher spatial frequencies of the object. Consequently, a higher imaging resolution is obtained in SWITSH compared to that of direct imaging with a diffractive lens. In the proof-of-concept study, a resolution improvement of an order was demonstrated. However, the optical architecture of the first version of SWITSH was not optimal, as the strength of the self-interference signal was weak. In this study, we improve SWITSH using different coded apertures, such as axicon and spiral element.An improvement in the strength of the self-interference signal was noticed with the axicon and spiral element. Simulation and experimental results using a diffractive lens, axicon and spiral element are presented.**

Keywords— super-resolution, diffractive lens, incoherent holography, coded aperture imaging, Lucy-Richardson-Rosen algorithm.

I. INTRODUCTION

Most of the properties of light, such as amplitude, phase and polarization, can be efficiently controlled using diffractive optical elements (DOEs), which work on the principles of diffraction [1]. The advantages of DOEs, such as compactness and lighter weight, make DOEs attractive replacements over traditional refractive elements [1, 2]. The complex optical beams generated by DOEs are useful for different applications, such as optical trapping, micro drilling and holography [1]. There are various lithographic methods, such as photo-lithography, e-beam lithography, ion beam lithography and femtosecond ablation, that can be used for manufacturing DOEs [1-3]. The above lithography techniques are suitable for different types of DOEs and therefore have different advantages and disadvantages when manufacturing a particular DOE configuration. For instance, photolithography has a resolution limit of ~ 2 μm but can

This research was funded by European Union's Horizon 2020 research and innovation agreement program grant No. 857627 (CIPHR).

create large area patterns at-a-time once the photomask is ready. Electron and ion beam lithography techniques can manufacture features < 100 nm, but the fabrication duration is significantly longer. Femtosecond ablation allows rapid fabrication but cannot fabricate features in the range of electron beam and focused ion beam lithography. A diffractive lens is one of the fundamental DOEs widely used for imaging applications. Large-area diffractive lenses are difficult to manufacture, irrespective of the type of manufacturing process. The m^{th} zone of a two-level diffractive lens for a focal length of f and wavelength λ has a radius $r_m = \sqrt{mf\lambda}$, the spacing between consecutive zones is given as $\Delta_m = \sqrt{mf\lambda} - \sqrt{(m-1)f\lambda}$. From the equation for spacing, it can be seen that as the zone number m and the spacing between the zones Δ_m are inversely proportional, and eventually for some value of m, the spacing Δ_m reaches the photo-lithography limit. To overcome this problem, one solution is to maintain the same period for all zones after the zone width reaches the photolithography limit. This solution may be effective for light collection, but it may not be ideal for imaging purposes due to spherical aberration [3]. To manufacture features beyond the limit of photo-lithography, either e-beam or ion-beam lithography can be adapted [3]. However, manufacturing DOEs with feature sizes of ~ 20 nanometers and with a size of 5 mm x 5 mm consumes several days. While manufacturing DOEs using electron beam lithography. effectively solves the problem except for the operating costs and prolonged manufacturing time, a new problem arises when large NA DOEs are manufactured. As per the relation between m and Δ_m, at some m, Δ_m reaches the photo-lithography limit. This problem can be solved by e-beam or ion-beam lithography, but after certain m, $\Delta_m \sim \lambda$. Once the $\Delta_m < \lambda$, undesirable polarization effects are created. Therefore, there is a fundamental problem in the manufacturing of large-area DOEs.

Recently, solutions were sought from indirect imaging concepts to obtain the resolution of large NA DOEs using small NA DOEs [4, 5]. A computational imaging technique Large-Area Diffractive lens with Integrated Sub-Apertures (LADISA) was invented [5]. In LADISA, instead of a single large NA diffractive lens, multiple small NA diffractive lenses with different linear phases were used such that all the image points are formed within the area of the image sensor. Therefore, LADISA creates several low-resolution images with a one-on-one correspondence between the low NA diffractive lenses and low-resolution images within the sensor instead of a single high-resolution image. The captured intensity distribution, for some cases, does not resemble the object due to the superposition of several object images. Even though the above-mentioned intensity distribution contains the higher spatial frequencies of the object the intensitydistribution does not directly reveal a high-resolution image. However, it is possible to recover the high-resolution image from the recorded intensity distribution using computational methods if the point spread function is known. There are many deconvolution methods, such as the matched, phase-only andinverse filters, the Wiener filter, and the Lucy-Richardson algorithm [6]. In 2022, a novel reconstruction method was developed by combining the Lucy-Richardson algorithm with non-linear reconstruction method developed by Rosen [6]. This new method is called the Lucy-Richardson-Rosen algorithm (LRRA). LRRA has been proven useful for a wide range of blurs [7]. The LADISA concept solved the problem of manufacturing large NA diffractive lenses to some extent. However, it requires manufacturing a large area device even though fine features are not needed.

A holographic solution was recently developed to solve the fundamental problem in manufacturing large area diffractive lenses. This innovation is labeled self-wavefront interference using transverse splitting holography (SWITSH) [8]. In SWITSH, the imaging resolution is improved from ~λ/NA_{DL} to ~~λ/NA_{IS}, where DL - diffractive lens and IS – image sensor. This SWITSH idea evolved based on the gap between the typical sizes of diffractive lenses and image sensors. In SWITSH, light focused by a small NA diffractive lens is allowed to diverge beyond the focal length and self-interfered with the light that detours the lens. The resulting hologram contains additional information about the object that corresponds to the higher spatial frequencies. Therefore, SWITSH, in addition to solving the problem associated with manufacturing large NA diffractive lenses, also enables 3D imaging capability. The preliminary studies of SWITSH using point objects reported in [8] demonstrated a resolution improvement of an order. One drawback in the use of SWITSH is that a substantial portion of the light incident on the low-NA diffractive lens remains uninvolved in self-interference. In this study, we proposed and demonstrated coded aperture-based SWITSH (CAB-SWITSH) to improve the self-interference of SWITSH. Since the goal of the research work is to achieve high resolution using a small area diffractive lens, there is no constraint in replacing the small area diffractive lens with another small area diffractive element as long as a high imaging resolution is obtained. In this study, two different coded apertures, such as an axicon and a spiral element, were used in place of the diffractive lens to redistribute the modulated light to the region where the light that detours the diffractive element is received. There are five sections in this paper. The design and the imaging procedure are explained in the methodology section. The third section contains the simulation results. The experimental studies are presented in the fourth section. The final section presents the summary and conclusion of the paper.

II. Methodology

The optical configuration of CAB-SWITSH is shown in Fig. 1. Light from an object point with an amplitude of $\sqrt{I_o}$ reaches the coded aperture located at a distance of z_1. The complex amplitude at the coded aperture is $\sqrt{I_o}C_1 Q\left(\frac{1}{z_1}\right) L\left(\frac{\bar{r_s}}{z_1}\right)$, where $L\left(\frac{\bar{s}}{z}\right) = exp\left[i2\pi(\lambda z)^{-1}\left(s_x x + s_y y\right)\right]$, $Q(a) = exp\left[i\pi a\lambda^{-1}R^2\right]$, C_1 is a complex constant and $R = \sqrt{x^2 + y^2}$. At the coded aperture, there is a transverse splitting of light, where part of the light is modulated by the coded aperture with a phase of $\Phi_c(x,y)$ and the light that detours the coded aperture propagates without any modulation. At the coded aperture plane, two apertures are as follows: $A_1 = \begin{cases} 1, R \le D_1/2 \\ 0, elsewhere \end{cases}$, where $D_1/2$ is the radius of the coded aperture and $A_2 = \begin{cases} 1, D_1/2 \le R < D_2/2 \\ 0, \ elsewhere \end{cases}$ where $D_2/2$ is the radius of the image sensor. The two optical fields generated at

the coded aperture are $\sqrt{I_o}C_1Q\left(\frac{1}{z_1}\right)L\left(\frac{\bar{r}_s}{z_1}\right)\Phi_c(x,y)A_1$ and $\sqrt{I_o}C_1Q\left(\frac{1}{z_1}\right)L\left(\frac{\bar{r}_s}{z_1}\right)A_2$. The point spread hologram I_{PSH} recorded at a distance of z_2 is given as

$$I_{PSH} = \left|\sqrt{I_o}C_1Q\left(\frac{1}{z_1}\right)L\left(\frac{\bar{r}_s}{z_1}\right)\{\Phi_c(x,y)A_1 + A_2\}\otimes Q\left(\frac{1}{z_2}\right)\right|^2$$

Where the symbol '$\otimes$' represents a 2D convolutional operator. There are two fields obtained at the image sensor, the modulated field containing lower spatial frequencies and the unmodulated field with both lower and higher spatial frequencies. When imaging using a small area diffractive lens in direct imaging mode, only the beam with lower spatial frequencies is used, so the resolution is low. However, with SWITSH and CAB-SWITSH, the higher spatial frequencies outside A_1 are also used for imaging. As the system is a linear and shift invariant system, the object hologram obtained for an object O is given as $I_{OH} = O\otimes I_{PSH}$. The image of the object with improved resolution can be obtained by processing I_{OH} with I_{PSH} using a deconvolution algorithm. Assuming z_1 is very large, the resolution is improved by a factor of ~D_2/D_1. Since our previous studies showed that the Lucy-Richardson-Rosen algorithm (LRRA) is superior to existing methods, the image is reconstructed as $I_R = I_{OH} \circledcirc^n_{\alpha,\beta} I_{PSH}$, where '$\circledcirc^n_{\alpha,\beta}$' represents the LRRA operator, and α, β and n are used to optimize the reconstruction result. A thorough investigation of the LRRA was provided in [10]. The schematic of LRRA is shown in Fig. 2.

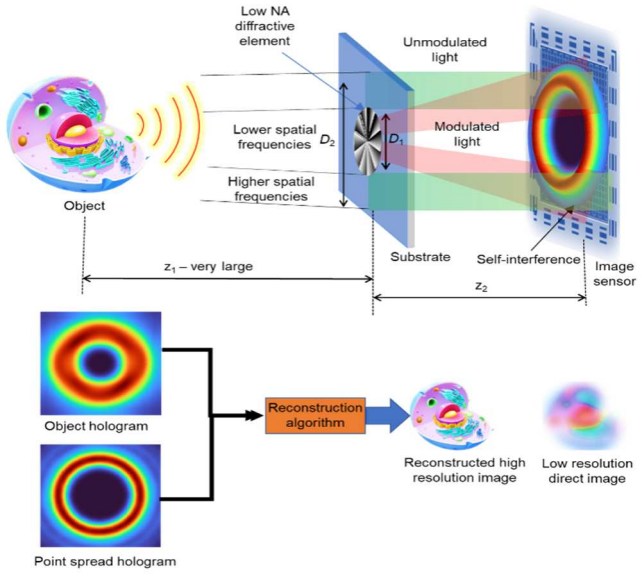

Fig. 1. Optical configuration of CAB-SWITSH

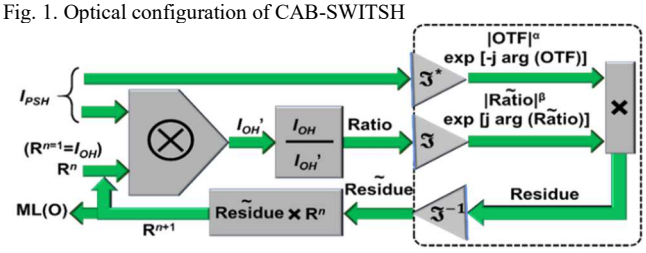

Fig. 2. Schematic of the Lucy-Richardson-Rosen algorithm

III. Simulation

The simulation studies were carried out in MATLAB with a matrix size of 500 pixels along the x and y directions, λ = 650 nm, pixel size of 10 µm, object distance z_1 of 1000 m and recording distance z_2 of 20 cm. The images of the coded aperture, I_{PSH}, I_{OH}, reconstructed results and the reference images of the test object and direct imaging results are shown in Fig. 3. Both SWITSH and CAB-SWITSH have better resolution than regular imaging using a small area diffractive lens. Another observation is that the high intensity peaks are present more in the case of CAB-SWITSH than SWITSH, indicating a better signal strength of the self-interference hologram.

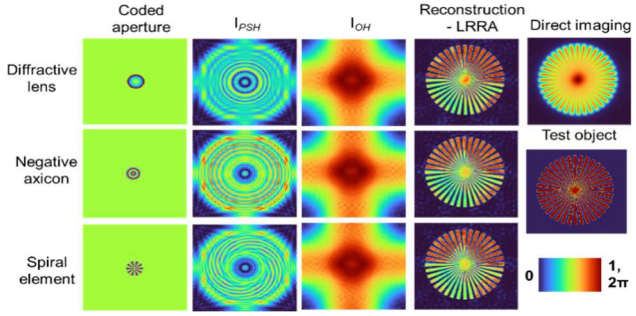

Fig. 3. Simulation results of direct imaging, SWITSH (first line) and CAB-SWITSH (second and third lines).

IV. Experiment

A photograph of the experimental setup is shown in Fig. 4. The setup consists of a high-power LED (Thorlabs, 940 mW, λ = 660 nm and Δλ = 20 nm), iris, polarizer, refractive lens, pinhole (50 µm), beam splitter, spatial light modulator (SLM) Thorlabs Exulus 4K1, 3840 × 2160 pixels, pixel size = 3.74 µm) and an image sensor (Zelux CS165MU/M 1.6 MP monochrome CMOS camera, 1440 × 1080 pixels with pixel size ~3.5 µm). To regulate the illumination, an iris is placed in front of the light source. Subsequently, the light undergoes polarization by passing through a polarizer that aligns with respect to the active axis of the SLM. The light from the object is collimated by a refractive lens of 5 cm focal length and passed through the beam splitter and incident on the SLM on which the coded phase masks were displayed on after the other, and the holograms were recorded by an image sensor. The PSH is captured using a pinhole with a diameter of 25 µm. In this study, the pinhole was moved to four different locations to produce a multipoint object and at each location, the hologram was recorded and they are summed to form the final hologram.

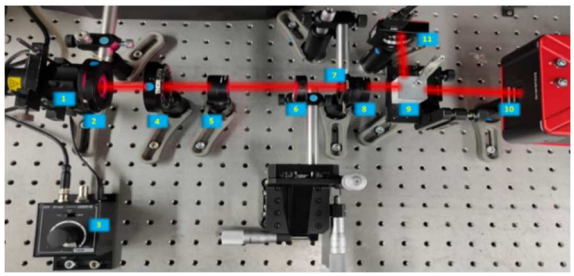

Fig. 4. Photograph of the experimental setup. The experimental setup consists of (1) LED (2) iris (3) LED power controller (4) polarizer (5) refractive lens (L1) (6) iris (7) object/pinhole (8) refractive lens (L2) (9) beam splitter (10) SLM (11) image sensor.

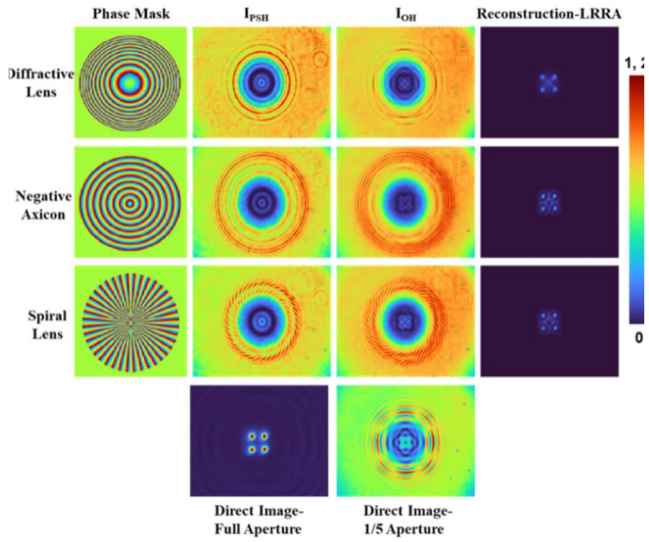

Fig. 5. Experimental results.

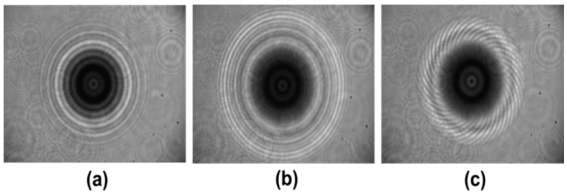

Fig. 6. Experimental results of (a) SWITSH and CAB-SWITSH (b) Axicon and (c) spiral element recorded using the same light input and exposure time of the image sensor.

The aperture was reduced to one-fifth of the total aperture, and the experiment was carried out. The reference image with a full aperture is also shown, which clearly shows four object points. With a smaller aperture, the four points cannot be resolved. However, with both SWITSH and CAB-SWITSH, the four points can be reconstructed. To compare the signal strength of the self-interference hologram between SWITSH and CAB-SWITSH, three holograms were recorded for each case but with the same light input and exposure time of the image sensor, as shown in Fig. 6. It can be seen from the results that there are more white regions in CAB-SWITSH compared to SWITSH, demonstrating an improvement in the signal strength of the self-interference hologram.

V. Conclusion

An improved version of SWITSH based on coded apertures has been proposed and demonstrated. This new CAB-SWITSH has better signal strength of self-interference holograms. In a way, CAB-SWITSH can be considered a generalization of SWITSH, where the DOE can be any element. In addition, changing from a diffractive lens to coded apertures offers better control of the beams and improved superposition. The preliminary results are promising. However, there are still many challenges associated with SWITSH, such as reconstruction noise, which will be solved in the future with improved reconstruction algorithms.

Acknowledgement

The authors thank the European Union's Horizon 2020 research and innovation programme.

References

[1] A. Vijayakumar and S. Bhattacharya, "Design and fabrication of diffractive optical elements with MATLAB," *SPIE Press*, 2017.

[2] J. Rosen, A. Vijayakumar and N. Hai, "Digital Holography Based on Aperture Engineering," *SPIE Digital Library,* 2023.

[3] A. Vijayakumar and S. Bhattacharya, "Characterization and correction of spherical aberration due to glass substrate in the design and fabrication of Fresnel zone lenses," *Applied Optics*, vol. 52, no. 24, pp. 5932–5932, Aug. 2013.

[4] J. Rosen, A. Vijayakumar, M. Kumar, M. R. Rai, R. Kelner, Y. Kashter, A. Bulbul and S. Mukherjee, "Recent advances in self-interference incoherent digital holography," *Advances in Optics and Photonics*, vol. 11, pp. 1-66, Feb. 2019.

[5] S. Gopinath, P. P. Angamuthu, T. Kahro, A. Bleahu, F. G. Arockiaraj, D. Smith, et al, "Implementation of a large-area diffractive lens using multiple sub-aperture diffractive lenses and computational reconstruction," *Photonics,* vol. 10, no. 1, pp. 3-3, Dec. 2022.

[6] A. Vijayakumar, M. Han, J. Maksimovic, S. H. Ng, T. Katkus et al, "Single-shot mid-infrared incoherent holography using Lucy-Richardson-Rosen algorithm," *Opto-Electronic Science*, vol. 1, no. 3, pp. 210006-1-210006-8, Jan. 2022.

[7] A. P. I. Xavier, F. G. Arockiaraj, S. Gopinath, A.S. J. F. Rajeswary, et.al., "Single-Shot 3D Incoherent Imaging Using Deterministic and Random Optical Fields with Lucy–Richardson–Rosen Algorithm," *Photonics*, vol. 10, no. 9, pp. 987, Aug. 2023.

[8] A. Bleahu, S. Gopinath, T. Kahro, S. H. Ng, K. Kukli, A. Tamm, S. Juodkazis, J. Rosen, A. Vijayakumar, "Self-wavefront interference using transverse splitting holography," *Results in Physics*, vol. 52, pp. 106839-106839, Sep. 2023